ONCOIMMUNOLOGY
2022, VOL. 11, NO. 1, e2131084 (14 pages)
https://doi.org/10.1080/2162402X.2022.2131084

Taylor & Francis
Taylor & Francis Group

ORIGINAL RESEARCH

OPEN ACCESS Check for updates

Targeting depletion of myeloid-derived suppressor cells potentiates PD-L1 blockade efficacy in gastric and colon cancers

Yao Tang, Cong Zhou, Qingli Li, Xiaojiao Cheng, Tinglei Huang, Fuli Li, Lina He, Baiweng Zhang, and Shuiping Tu

State Key Laboratory of Oncogenesis and Related Genes, Department of Oncology, Renji Hospital, Shanghai Jiao Tong University, School of Medicine, Shanghai, China

ABSTRACT

Myeloid-derived suppressor cells (MDSCs) have been demonstrated to *suppress antitumor immunity* and induce resistance to PD-1/PD-L1 blockade immunotherapy in gastric and colon cancer patients. Herein, we found that MDSCs accumulate in mice bearing syngeneic gastric cancer and colon cancer. Death receptor 5 (DR5), a receptor of TNF-related apoptosis-inducing ligand (TRAIL), was highly expressed on MDSCs and cancer cells; targeting DR5 using agonistic anti-DR5 antibody (MD5-1) specifically depleted MDSCs and induced enrichment of $CD8^+$ T lymphocytes in tumors and exhibited stronger tumor inhibition efficacy in immune-competent mice than in T-cell-deficient nude mice. Importantly, the combination of MD5-1 and anti-PD-L1 antibody showed synergistic antitumor effects in gastric and colon tumor-bearing mice, resulting in significantly suppressed tumor growth and extended mice survival, whereas single-agent treatment had limited effect. Moreover, the combination therapy induced sustained memory immunity in mice that exhibited complete tumor regression. The enhanced antitumor effect was associated with increased intratumoral $CD8^+$ T-cell infiltration and activation, and a more vigorous tumor-inhibiting microenvironment. In summary, our findings highlight the therapeutic potential of combining PD-L1 blockade therapy with agonistic anti-DR5 antibody that targets MDSCs in gastric and colon cancers.

ARTICLE HISTORY
Received 25 June 2022
Revised 13 September 2022
Accepted 27 September 2022

KEYWORDS
Myeloid-derived suppressor cells; death receptor 5; PD-L1; gastric cancer; colon cancer; immunotherapy

Introduction

Cancer immunotherapy has made significant breakthroughs in the field of cancer treatment and is becoming one of the main therapeutic approaches for patients with various cancers.[1,2] The PD-1/PD-L1 pathway plays a pivotal role in cancer immune evasion by inhibiting the antitumor activity of T cells. Therapeutic antibodies that block the interaction of PD-1/PD-L1 can induce robust and durable antitumor immune responses in patients with solid tumors, including gastric cancer and colon cancer. However, the therapeutic benefits are restricted to a subset of gastric and colon cancer patients,[3,4] indicating the involvement of other immune suppression mechanisms.

Myeloid-derived suppressor cells (MDSCs) are one of the main immune suppressive populations in the tumor microenvironment (TME). These cells induce tumor immune escape by suppressing the proliferation and activation of cytotoxic T cells and are considered a major obstacle to effective cancer immunotherapy.[5,6] Targeting inhibition of MDSCs is now emerging as a promising strategy to maximize and extend the benefits of PD-1/PD-L1 blockade therapy for cancer treatment.[7–9] Many agents, such as all-trans retinoic acid, CSF-1 receptor inhibitor, anti-Gr-1 antibody, etc., have shown the capacities to alleviate the immune suppression caused by MDSCs and enhance antitumor immunity,[10–12] however, most of these agents lack specificity for MDSCs.

Death receptor 5 (DR5) is one of the receptors of TNF-related apoptosis-inducing ligand (TRAIL) that can induce cell death by transducing the pro-apoptotic signal.[13] It is frequently expressed on the surface of cancer cells, making DR5 a desirable target for antitumor therapy.[14] Up to now, agonistic antibodies that target DR5 have exhibited excellent antitumor efficacy in various murine tumor models and are being tested in clinical trials for cancer treatment.[15,16] Despite its amplification in cancer cells, DR5 was also shown to be highly expressed on MDSCs in tumor-bearing mice, and agonistic anti-DR5 antibodies could specifically eliminate MDSCs in tumor-bearing mice and cancer patients,[17,18] providing a rationale to combine these agents with PD-1/PD-L1 blockade therapies. However, to the best of our knowledge, there has not been any published literature demonstrating the combination effects of these agents for gastric and colon cancer therapy *in vivo*. Moreover, the associated toxicity of this form of combination therapy is unknown.

In this study, we demonstrated that MDSCs accumulated in the syngeneic murine gastric and colon cancer models and expressed high levels of DR5. Targeting DR5 using MD5-1 (an agonistic antibody to mouse DR5) could selectively deplete MDSCs and promote T-cell antitumor response. Importantly, the combination of MD5-1 and anti-PD-L1 had superior therapeutic efficacy against gastric and colon tumors and remarkably extended survival of mice. Meanwhile, anti-PD-L1 or

CONTACT Shuiping Tu tushuiping@yahoo.com State Key Laboratory of Oncogenesis and Related Genes, Department of Oncology, Renji Hospital, Shanghai Jiao Tong University, School of Medicine, Shanghai, China
Supplemental data for this article can be accessed online at https://doi.org/10.1080/2162402X.2022.2131084

MD5-1 monotherapy only had a little or moderate antitumor effect. Notably, in mice bearing MFC gastric tumors, the combination therapy resulted in 40% of tumor eradication and induced durable tumor-specific immune memory in these mice. The enhanced antitumor effect of combination therapy was associated with increased intratumoral $CD8^+$ T-cell infiltration and activation, and a stronger tumor-inhibiting microenvironment. Thus, the combination of agonistic anti-DR5 antibody and an anti-PD-L1 antibody may serve as a promising strategy for gastric and colon cancer immunotherapy.

Materials and methods

Mice and cell lines

The murine forestomach cancer cell line (MFC, derived from 615 mice) and murine colon cancer cell line (MC38, derived from C57BL/6 mice) were purchased from the Chinese Academy of Sciences (Shanghai, China). Cells were cultured in custom RPMI 1640 (Gibco) supplemented with 10% fetal bovine serum and 1% pen/strep (Gibco) in a 37°C and 5% CO_2 incubator. 615 mice (5–7-week old, female) were purchased from the animal facility of the State Key Laboratory of Experimental Hematology (Tianjin, China). BALB/c nude mice and C57BL/6 mice (5–7-week old, female) were obtained from SLAC Laboratory Animal Co. Ltd (Shanghai, China). Animals were kept in a specific pathogen free (SPF) room with optimal light cycle, temperature, and humidity and free access to food and water supply.

Tumor models and treatments

To establish tumor xenograft models, 1×10^6 MFC cells were inoculated s.c. into the flank of syngeneic 615 mice or BALB/c nude mice; 5×10^5 MC38 cells were inoculated s.c. into the flank of C57BL/6 mice. Treatment commenced on d 7 after tumor inoculation when the mean tumor volume reached about 80 mm^3-100 mm^3. Tumor-bearing mice were injected i.p. with MD5-1 (50 μg/mouse) or anti-PD-L1 mAb (200 μg/mouse, clone 10 F.9G2) or their combination or control IgG (Armenian hamster IgG, clone N/A and rat IgG2b, Clone LTF-2) every 3 d for 3 times in total, respectively. All antibodies were obtained from Bio X Cell. Tumors were measured every 3 d. Tumor volume was calculated as length×width^2/2 (mm^3). TGI (tumor growth inhibition rate) was calculated by the following formula: $[(C_t - C_0) - (T_t - T_0)]/(C_t - C_0) \times 100$, where C_t or T_t = the mean tumor volume of control or treatment group at time (t), C_0 or T_0 = the mean tumor volume of control or treatment group at treatment initiation. Mice were humanely euthanized when tumor size reached 20 mm in major diameter. No visible and palpable tumors observed in mice for 3 months after receiving the last injection of MD5-1 plus anti-PD-L1 combination therapy were defined as complete regression (CR). At the endpoint, peripheral blood serum samples were collected for evaluation of the liver, renal, and heart function.

For re-challenge study, mice with CR of MFC tumors were inoculated s.c. with 2×10^6 MFC cells. As a control, age-matched naïve 615 mice were injected s.c. with the same amount of MFC cells. All animal experiments were approved by the Animal Care and Use Committee at the Renji Hospital affiliate of Shanghai Jiao Tong University.

Tissue processing and flow cytometry

Spleens were processed by mechanical trituration following red blood cell lysis. Tumors were minced with scissors and incubated for 1 hour at 37°C for digestion in custom RPMI 1640 containing 1 mg/mL collagenase IV (Sigma) and 0.1 mg/mL DNase I (Roche). Cell suspensions were filtered through a 70-mm strainer, washed with PBS, and stained with Fixable Viability Dye for 30 mins at 4°C (eBioscience). Cells were then incubated with anti-CD16/32 mAb (clone 2.4G2) to block Fc receptors at 4°C for 15 mins. Finally, cell suspensions were stained with fluorescence-conjugated anti-mouse antibodies for cell surface markers, including CD45 (clone 30-F11), CD11b (clone M1/70), Gr-1 (clone RB6-8C5), DR5 (clone MD5-1), PD-L1 (clone 10 F.9G2), CD4 (clone RM4-5), CD8a (clone 53–6.7), PD-1 (clone 29 F.1A12), MHC Class II (I-A/I-E) (clone M5/114), CD11c (clone N418), and F4/80 (clone BM8).

For nuclear protein FoxP3 staining, cells were then fixed in fixation/permeabilization buffer (eBioscience) and stained with antibody against mouse Foxp3 (clone R16-715). For intracellular IFN-γ and TNF-α staining, the isolated cells were stimulated with leukocyte activation cocktail in the presence of Golgistop (BD Biosciences) at 37°C for 4 hours. After being stained with Fixable Viability Dye and surface markers, cells were permeabilized using permeabilization buffer (eBioscience) and then stained with anti-mouse IFN-γ (clone XMG 1.2) and TNF-α (clone MP6-XT22) antibodies. All antibodies were purchased from BD Biosciences or BioLegend. Flow cytometry was performed on LSRFortessa (BD Bioscience), and data were analyzed using FlowJo software.

MDSC and T cell isolation

Single-cell suspensions of the spleens from tumor-bearing 615 mice were sorted on Super MACS separator (MiltenyiBiotec) using mouse Myeloid-Derived Suppressor Cell Isolation Kit (MiltenyiBiotec) for gMDSCs and mMDSCs according to manufacturer's protocol or sorted by FACSAria Cell Sorter (BD Biosciences) for $CD3^+$ T cells.

MDSC adoptive transfer

Single-cell suspensions were prepared from bone marrow of tumor-bearing 615 mice, and total MDSCs ($CD11b^+Gr\text{-}1^+$) were sorted via FACSAria Cell Sorter (BD Biosciences). 5×10^6 bone marrow-derived MDSCs were injected intravenously into tumor-bearing 615 mice one hour after each MD5-1 treatment (3 injections in total).

Apoptosis assays

To evaluate MD5-1-mediated killing, MFC and MC38 cells (1×10^5), isolated splenic MDSCs (2×10^5, supplemented

with 10 ng/ml GM-CSF), or $CD3^+$ T cells (2×10^5) were cultured in plates (24-well plate, Corning) pre-coated with Protein A (10 μg/ml, Pierce) followed by coating with MD5-1 or control IgG for 24 hours. Cells were washed twice in PBS, stained with FITC-Annexin V and propidium iodide (PI) according to manufacturer's protocol (BD PharMingen) and analyzed by flow cytometry immediately.

Immunohistochemistry and TUNEL staining

At the time of sacrifice, tumors were harvested and fixed in 4% paraformaldehyde for 24 hours. Fixed samples were embedded in paraffin and cut into 4 μm sections. The sections were deparaffinized in xylene and rehydrated with graded alcohol and then placed in 3% H_2O_2 to block endogenous peroxidase activity. After being boiled in 1 mM EDTA (pH 9.0) for antigen retrieval and blocked with 5% goat serum, sections were incubated with antibodies against mouse CD3 (ab16669, 1:150, Abcam) and Ki67 (ab15580, 1 μg/ml, Abcam) overnight at 4°C. After washing with PBS, sections were incubated in EnVision secondary antibody (Dako) for 30 mins at room temperature. Immunoreactivity was visualized with DAB (Beyotime Biotechnology). The sections were counterstained with hematoxylin. Tumor, lung, heart, liver, spleen, and kidney were also collected for histological analysis using hematoxylin and eosin (H&E) staining.

For TUNEL staining, the deparaffinized and rehydrated tissue sections were incubated in 20 g/ml proteinase K (Millipore) for 15 mins at room temperature. After being washed in PBS, the sections were stained using the ApopTag Fluorescein *in situ* Apoptosis Detection Kit (Millipore) according to the manufacturer's (Millipore) protocol. DAPI (1.0 μg/mL) was used for nuclear counterstain.

Statistical analysis

Statistical analysis was performed using Prism7 (GraphPad Software). Data are presented as mean ± SEM. Statistical analysis between two experimental groups was performed using a two-tailed *t* test. One-way ANOVA was used for the comparisons of three or four experimental groups. Tumor measurements and TGI were analyzed using 2-way ANOVA. Survival curves were plotted using Kaplan–Meier method. Differences in survivals were determined using Log-Rank (Mantel-Cox) analysis. *p* values less than 0.05 were considered statistically significant.

Data availability

The data used and/or analyzed during the current study are available from the corresponding author on reasonable request.

Results

MDSCs accumulate in mice bearing gastric and colon tumors and exhibit high DR5 expression

Many studies have demonstrated that MDSC level is elevated in the peripheral blood and tumor tissues of patients with gastric or colon cancer.[19–21] As expected, spleens and tumor tissues in MFC gastric tumor and MC38 colon tumor-bearing mice exhibited robust accumulation of total MDSCs ($CD11b^+$ $Gr\text{-}1^+$) compared to spleens in corresponding naïve mice (Figure 1a**&b**). MDSCs in mice bearing MC38 tumors have been fully characterized in several studies.[22,23] In mice bearing MFC tumors, increase of granulocytic (gMDSCs, $CD11b^+Ly6G^+Ly6C^{low}$) and monocytic (mMDSCs, $CD11b^+Ly6G^-Ly6C^{high}$) MDSC subsets both contributed substantially to the accumulation of total MDSCs (Figure 1c). The ratios of gMDSCs to mMDSCs in spleens and tumors were approximately 3.6:1 and 2.3:1, respectively (**Supplementary Fig. 1**). Notably, frequencies of gMDSCs and mMDSCs were both markedly higher in tumor tissue than those in spleen of the same mice (Figure 1c), indicating that MDSCs are preferentially recruited to the tumor than to the spleen.

A previous study by Condamine *et al.* showed that DR5 is expressed on MDSCs.[17] Accordingly, upregulation of surface DR5 was detected in splenic and tumor-infiltrating MDSCs of both murine tumor models (Figure 1d). In MFC tumor-bearing mice, both gMDSCs and mMDSCs in spleens and tumors exhibited markedly increased DR5 expression compared with their respective counterparts in spleens of naive mice (Figure 1e**, Supplementary Fig. 2A**). Notably, DR5 level was significantly higher in both MDSC subsets from tumors than those from spleens (Figure 1e). In tumor tissue, upregulation of DR5 was more prominent in mMDSCs than in gMDSCs. The percentages of DR5 positive gMDSCs and mMDSCs were 53% ± 3.4% and 77% ± 6.1%, respectively (**Supplementary Fig. 2B&C**). In addition, we observed a substantially increased PD-L1 expression on tumor-infiltrating gMDSCs and mMDSCs, which is an indicator of their immunosuppressive activity (**Supplementary Fig. 3A&B**). Thus, MDSCs that express high levels of DR5 accumulate in the spleens and tumors of MFC and MC38 tumor-bearing mice. DR5 may serve as a target to deplete MDSCs in the treatment of MFC and MC38 tumors.

Agonistic anti-DR5 antibody selectively depletes MDSCs

To evaluate whether targeting DR5 can effectively deplete MDSCs, we first examined the capacity of MD5-1 to induce MDSC apoptosis *in vitro*. The gMDSCs and mMDSCs were isolated from the spleens of MFC tumor-bearing mice and cultured in the presence of MD5-1 or control IgG. When cultured *in vitro*, freshly sorted MDSCs usually undergo rapid and spontaneous death; thus, we detected certain cell apoptosis in both MDSC subsets cultured with control IgG. In contrast, treatment with MD5-1 significantly increased the frequencies of apoptotic cells (Annexin V^+) in both gMDSCs (10 μg/ml of MD5-1) and mMDSCs (1 and 10 μg/ml of MD5-1) (Figure 2a). Given that T cells are the main antitumor effector cells, the direct effect of MD5-1 on $CD3^+$ T cells was determined. We found no significant difference in the frequencies of apoptotic cells between $CD3^+$ T cells that incubated with control IgG and varying concentrations of MD5-1 (Figure 2b), indicating that MD5-1 is not cytotoxic to T cells.

We then determined the MDSC-depleting effect of MD5-1 *in vivo*. Mice bearing MFC tumors were treated with one

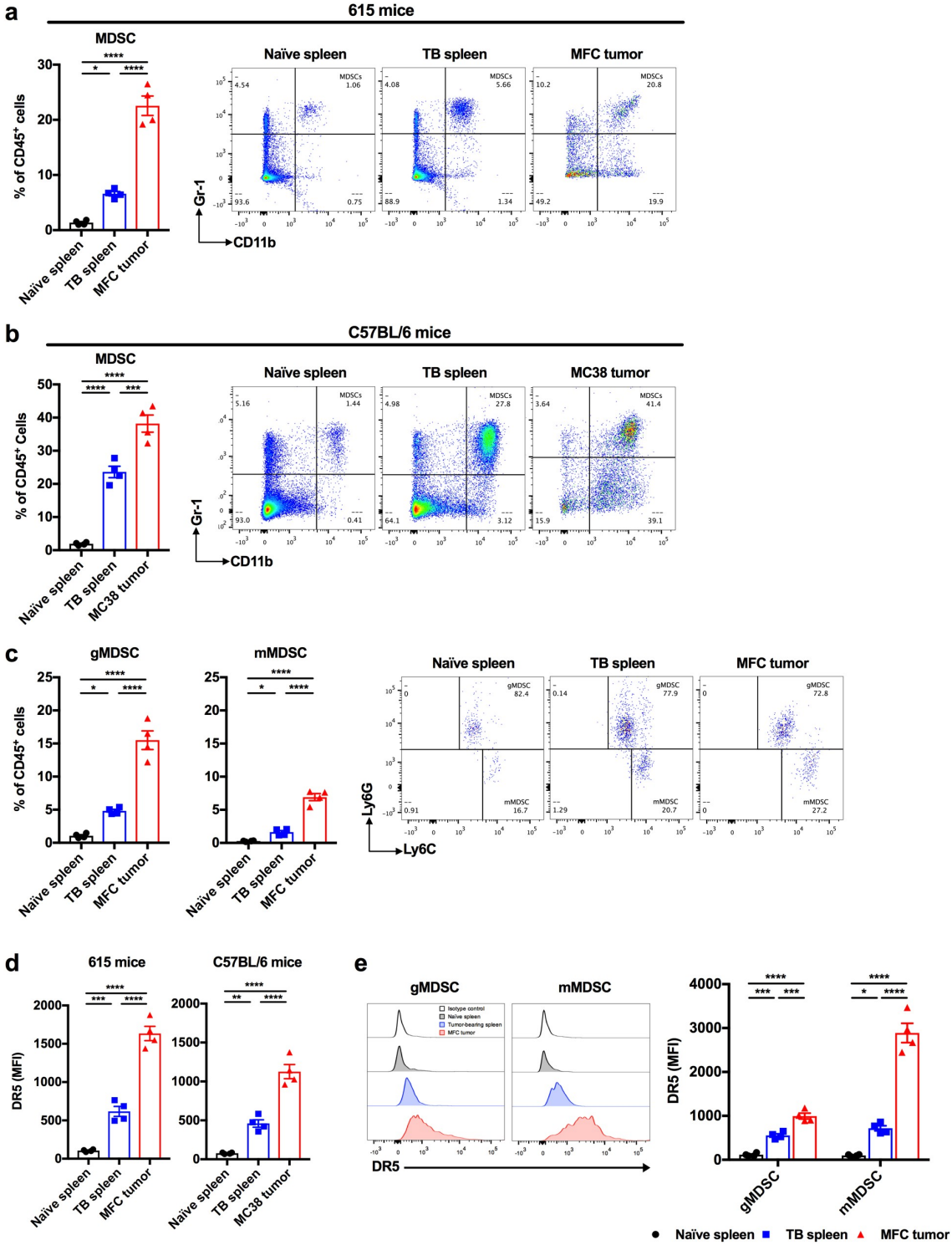

Figure 1. MDSCs accumulate in the spleens and tumors of MFC and MC38 tumor-bearing mice and exhibit high DR5 expression. 615 and C57BL/6 mice were subcutaneously inoculated with MFC and MC38 cells, respectively. On d 7 after inoculation, spleens and tumors were harvested from tumor-bearing mice and subjected to flow cytometry analysis for MDSCs. (a, b) Left, percentages of total MDSCs ($CD11b^+Gr\text{-}1^+$) in live, $CD45^+$ cells from spleens (TB spleen) and tumors of MFC tumor-bearing 615 mice (a) or MC38 tumor-bearing C57BL/6 mice (b) and spleens of their respective naive mice. Right, representative flow cytometry dot plots of total MDSCs gated on live, $CD45^+$ cells. (c) Left, percentages of gMDSCs ($Ly6G^+Ly6C^{low}$) and mMDSCs ($Ly6G^-Ly6C^{high}$) in live, $CD45^+$ cells. Right, representative dot plots of gMDSCs and mMDSCs gated on total MDSCs. (d) Quantitative mean fluorescence intensity (MFI) of DR5 on total MDSCs in mice bearing MFC tumors (left) or MC38 tumors (right). (e) Left, histograms of DR5 expression on gMDSCs and mMDSCs. Right, MFI of DR5 on gMDSCs and mMDSCs were quantified. $n = 4$ mice/group. Results are representative of 3 independent experiments. Data are shown as mean ± SEM. p values were obtained by one-way ANOVA, followed by Tukey's multiple comparisons test, $^*p < .05$, $^{**}p < .01$, $^{***}p < .001$, $^{****}p < .0001$.

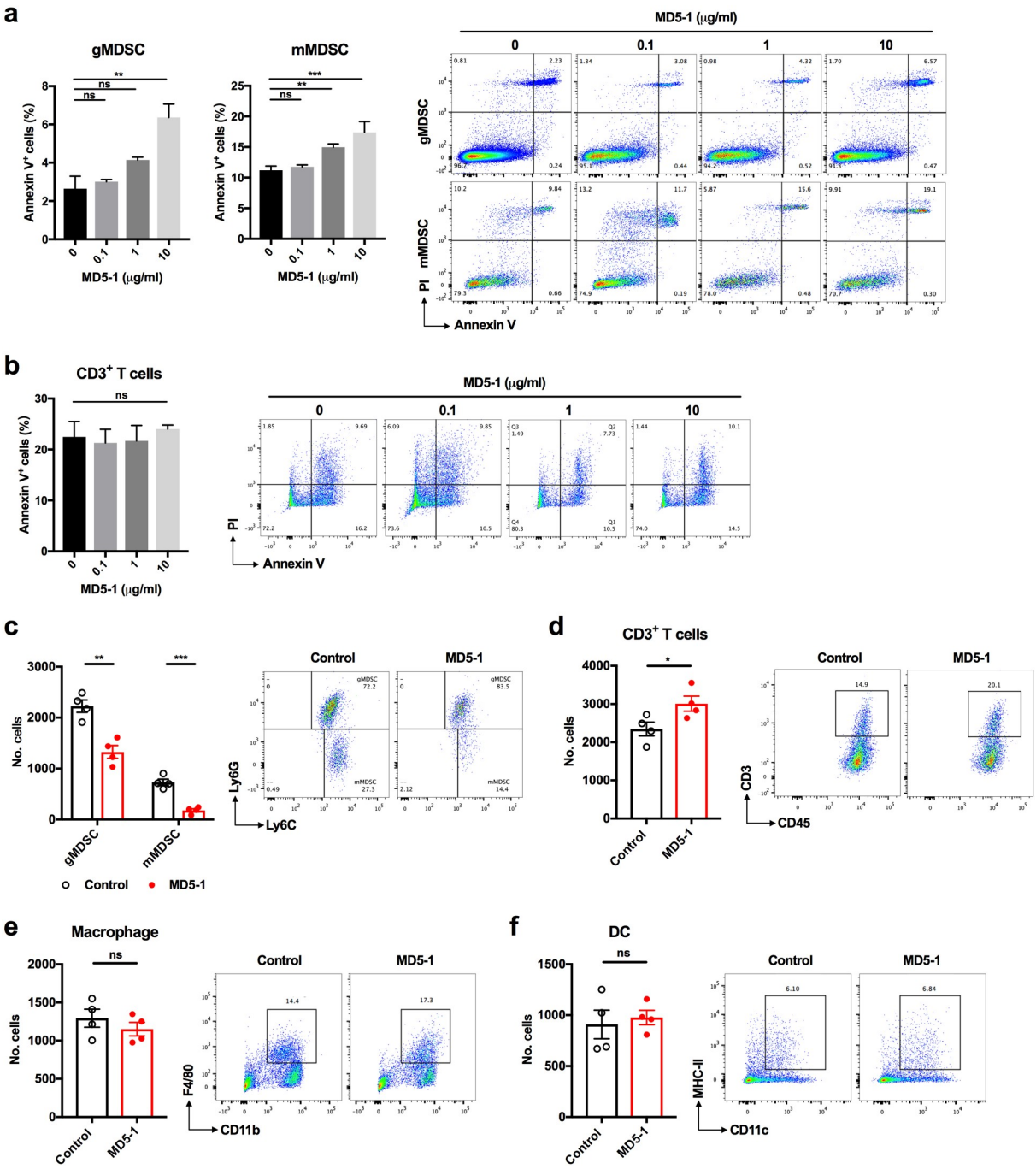

Figure 2. MD5-1 specifically deletes MDSCs in tumors. (a, b) Freshly isolated MDSC subsets (a) and $CD3^+$ T cells (b) were cultured in plates coated with varying concentrations of MD5-1 or control IgG (0, 0.1, 1 and 10 μg/ml) for 24 hours. Left, percentages of Annexin V^+ cells in gMDSCs, mMDSCs and T cells were determined. Right, representative dot plots of cell apoptosis analysis. (c) 14 d after MFC tumor inoculation (tumor volume ≈ 400 mm^3), tumor-bearing mice were treated with one dosage of MD5-1 or control IgG (50 μg/mouse, $n = 4$ mice/group). Left, the absolute number of gMDSCs and mMDSCs (per 6×10^4 live cells) in tumors were determined by flow cytometry analysis. Right, representative dot plots. (d-f) Absolute number of $CD3^+$ T cells (d), macrophages (e) and DCs (f) in tumors were determined (left) and representative FACS plots (right) are shown. Results are representative of 3 independent experiments. Data are shown as mean ± SEM. p values were obtained by unpaired student's t test, $^*p < .05$, $^{**}p < .01$, $^{***}p < .001$, ns, not significant.

dosage of MD5-1 or control IgG. Twenty-four hours after the injection, MDSCs in tumor tissues and spleens of treated mice were examined. As expected, MD5-1 treatment significantly decreased the accumulation of gMDSCs and mMDSCs in both tumors and spleens. In tumors, MD5-1 reduced the absolute number of gMDSCs and mMDSCs by about 40.4% and 75.6%, respectively, and in spleens, by about 25.7% and 33.6%, respectively (Figure 2c, **Supplementary Fig. 4**). Additionally, we observed a slight but significant increase in $CD3^+$ T cells in MD5-1 treated tumors (Figure 2d), which was likely resulted from reduced MDSC burden. Meanwhile, MD5-1 did not affect the presence of other intratumoral myeloid cell populations (macrophages and dendritic cells) (Figure 2e&f). Altogether, these data demonstrated that MD5-1 can selectively deplete MDSCs in the tumor bed and spleen of tumor-bearing mice.

MD5-1-mediated MDSC depletion promotes T-cell infiltration and contributes to tumor suppression

DR5 is expressed in various types of cancer cells. We found that both MFC and MC38 cells expressed high levels of DR5 (**Supplementary Fig. 5A**). A high dose of MD5-1 induced apoptosis in around 60% of MFC cells and 27% of MC38 cells *in vitro* experiments (**Supplementary Fig. 5B&C**), suggesting that MD5-1 may directly inhibit tumor growth *in vivo*, independent of its MDSC depleting effect. Given that reduction of MDSC burden can lead to reinvigoration of T-cell antitumor responses, we evaluated the contribution of T cells to the antitumor efficacy of MD5-1. The tumor inhibition effect of MD5-1 was compared in MFC tumors in T-cell-deficient nude mice and immune-competent 615 mice. While MD5-1 treatment effectively suppressed tumor growth and increased the survival of tumor-bearing nude mice (Figure 3a**&b**), it exhibited significantly stronger tumor-inhibiting efficacy and resulted in better survival in tumor-bearing 615 mice (Figure 3c-f). These results demonstrate that the T-cell-mediated antitumor response contributed to the enhanced tumor suppression effect of MD5-1.

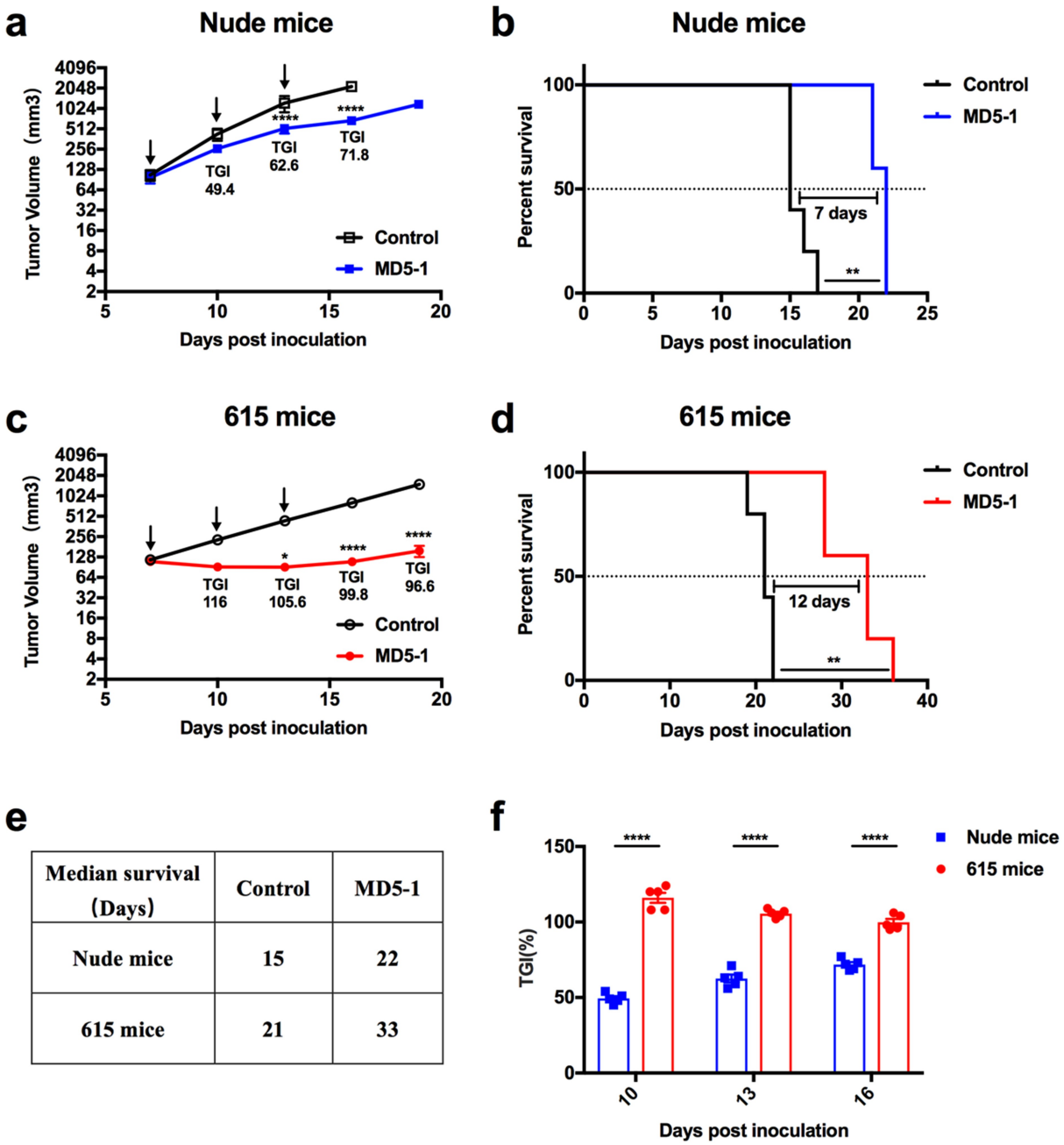

Median survival (Days)	Control	MD5-1
Nude mice	15	22
615 mice	21	33

Figure 3. T cells contributes to MD5-1-mediated tumor inhibition. T-cell-deficient nude mice and 615 mice were s.c. inoculated with 1×10^6 MFC cells simultaneously and treated with MD5-1 or control IgG (50 μg/mouse) on d 7, 10 and 13 after tumor implantation, tumor volume and mice survival were observed (n = 5 mice/group). (a, b) Tumor growth curves (a) and survival curves (b) of T-cell-deficient nude mice. (c, d) Tumor growth curves (d) and survival curves (d) of 615 mice. (e) Median survival of tumor-bearing nude mice and 615 mice treated with MD5-1 or control IgG. (f) Tumor growth inhibition rate (TGI) was compared between nude mice and 615 mice. Results are representative of at least 2 independent experiments. Tumor volume and TGI were compared using 2-way ANOVA with Bonferroni multiple comparison test. Survival curves were analyzed via Mantel-Cox log-rank test. *$p < .05$, **$p < .01$, ****$p < .0001$.

To further characterize alterations in the immune microenvironment after MD5-1 treatment, T cells and MDSCs of treated tumor-bearing 615 mice were analyzed. In line with the conclusion *in vivo*, MD5-1 administration markedly enhanced the infiltration of $CD8^+$ T cells in the tumor tissues and increased the frequencies of both $CD8^+$ and $CD4^+$ T cells in the spleens of tumor-bearing 615 mice (Figure 4a). Semi-quantitative immunohistochemistry (IHC) also showed that MD5-1 treated tumors had a remarkably higher T-cell infiltration in both the tumor periphery and tumor center compared to control IgG treated tumors (Figure 4b&c). Moreover, the proportions of MDSCs in tumors and spleens were also significantly decreased following MD5-1 treatment (Figure 4d).

The increased T-cell infiltration could also be a secondary result of the direct tumor killing effect of MD5-1 since smaller tumors usually have less immune suppressive MDSCs. Thus,

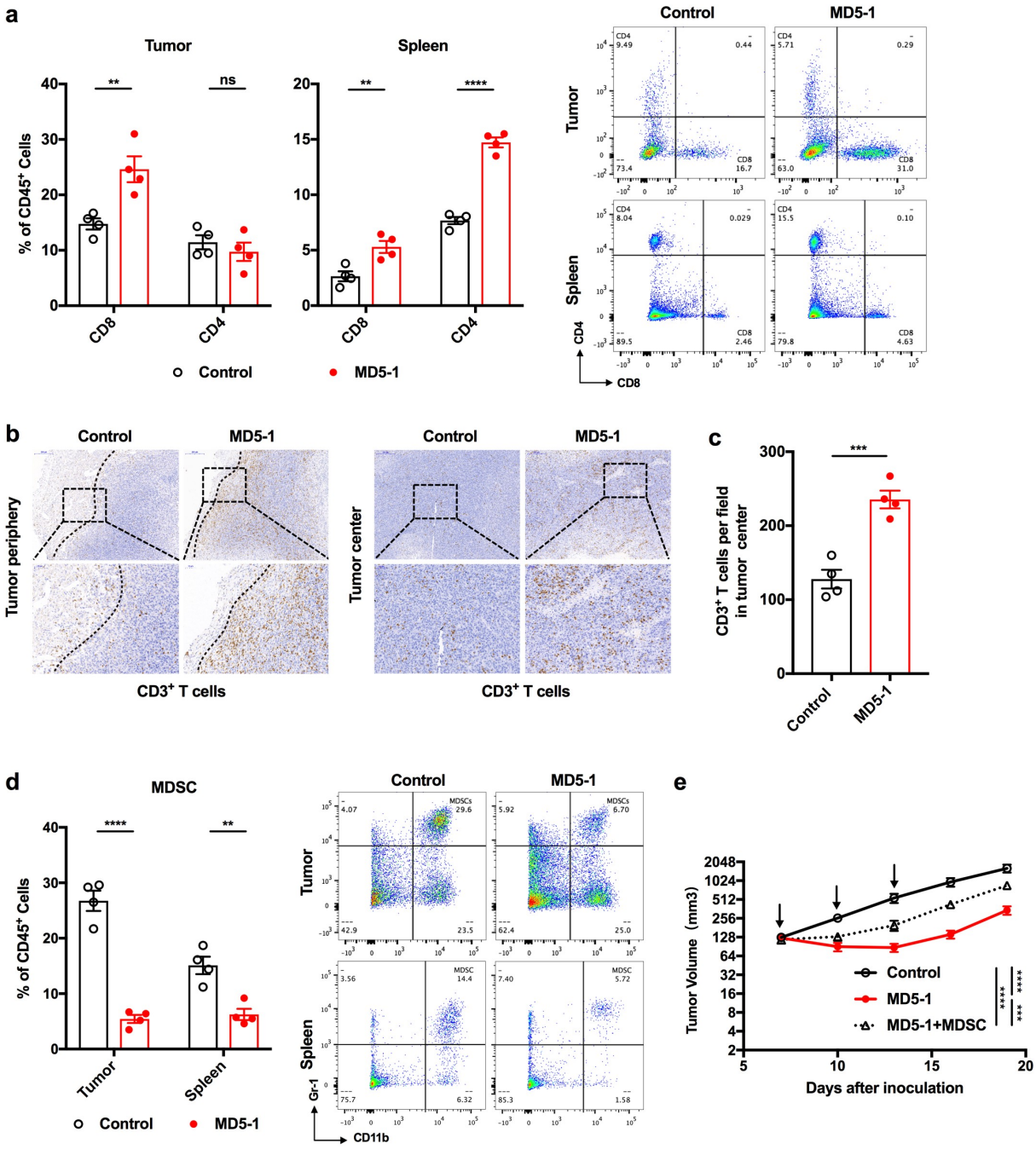

Figure 4. T-cell enrichment and MDSC depletion contribute to the antitumor effect of MD5-1. (a) 7 d after 3 injections of MD5-1 or control IgG (50 μg/mouse), tumors and spleens of treated 615 mice were collected for T cells and MDSCs examination (n = 4 mice/group). Left, proportion of $CD8^+$ and $CD4^+$ T cells (in $CD45^+$cells) in tumors and spleens. Right, representative dot plots gated on live, $CD45^+$ cells. (b) Representative CD3 staining (brown) of tumor periphery (left) and center (right). Dashed lines indicate tumor boundaries. Scale bar, 200 μm (left), 50 μm (right). (c) Quantification of infiltrating $CD3^+$ T lymphocytes in tumor center (positive cell number per field). (d) Left, proportion of total MDSCs (in $CD45^+$ cells) in tumors and spleens. Right, representative dot plots gated on live, $CD45^+$ cells. (e) Tumor growth curves of MFC tumors that received different treatment. Black arrows indicate treatment and MDSC adoptive transfer times. Results are representative of 3 independent experiments. Data are shown as mean ± SEM. *p* values were obtained by unpaired student's *t* test, $^{**}p < .01$, $^{***}p < .001$, $^{****}p < .0001$, ns, not significant.

we further evaluated the contribution of MDSC elimination to the effect of MD5-1 on tumor growth. Isolated total MDSCs were intravenously transferred into tumor-bearing 615 mice after each MD5-1 injection. As expected, adoptive transfer of MDSCs markedly compromised the antitumor activity of MD5-1 (Figure 4e), indicating that reduction of MDSCs is necessary for the antitumor efficacy of MD5-1. Overall, MD5-1-mediated MDSC depletion induces T-cell infiltration and is essential for its tumor suppression effect.

Combination of MD5-1 and anti-PD-L1 antibody enhances antitumor effects and prolongs *survival* of MFC and MC38 tumor–bearing mice

Given that MD5-1 treatment reduced MDSC burden and enhanced T-cell infiltration, we hypothesized that MD5-1 could render the tumors more responsive to PD-L1 blockade therapy. The combination regimen of MD5-1 and anti-PD-L1 antibody were then tested in MFC and MC38 tumor-bearing mice. We found that around 19.5% of MFC cells and 12.2% of MC38 cells express PD-L1 (**Supplementary Fig. 6**). Anti-PD-L1 antibody alone had a moderate effect on the growth of established MFC tumors. Consistent with the *in vivo* observation in Figure 3, MD5-1 considerably inhibited MFC tumor growth. Remarkably, the combination of MD5-1 and anti-PD-L1 antibody effectively reduced the tumor burden (Figure 5a**&**b) and significantly prolonged the survival of MFC tumor-bearing mice (Figure 5c). Moreover, the combination treatment led to complete tumor regression in 2 out of 5 MFC tumors (complete response, CR = 40%) and effectively retarded the growth of three other tumors. Meanwhile, no complete tumor regression was observed in MD5-1 or anti-PD-L1 monotherapy group (Figure 5d**&**e). In accordance with the enhanced antitumor effect, the combination of MD5-1 and anti-PD-L1 antibody significantly enhanced necrosis in the tumor center, markedly increased apoptosis, and reduced proliferation of the tumor cells in non-necrotic tumor areas compared to either monotherapy, as confirmed by H&E, TUNEL, and Ki67 staining, respectively (**Supplementary Fig. 6A-C**). In MC38 tumor-bearing mice, both MD5-1 and anti-PD-L1 monotherapies had limited effects on the tumor growth. In contrast, MD5-1 combined

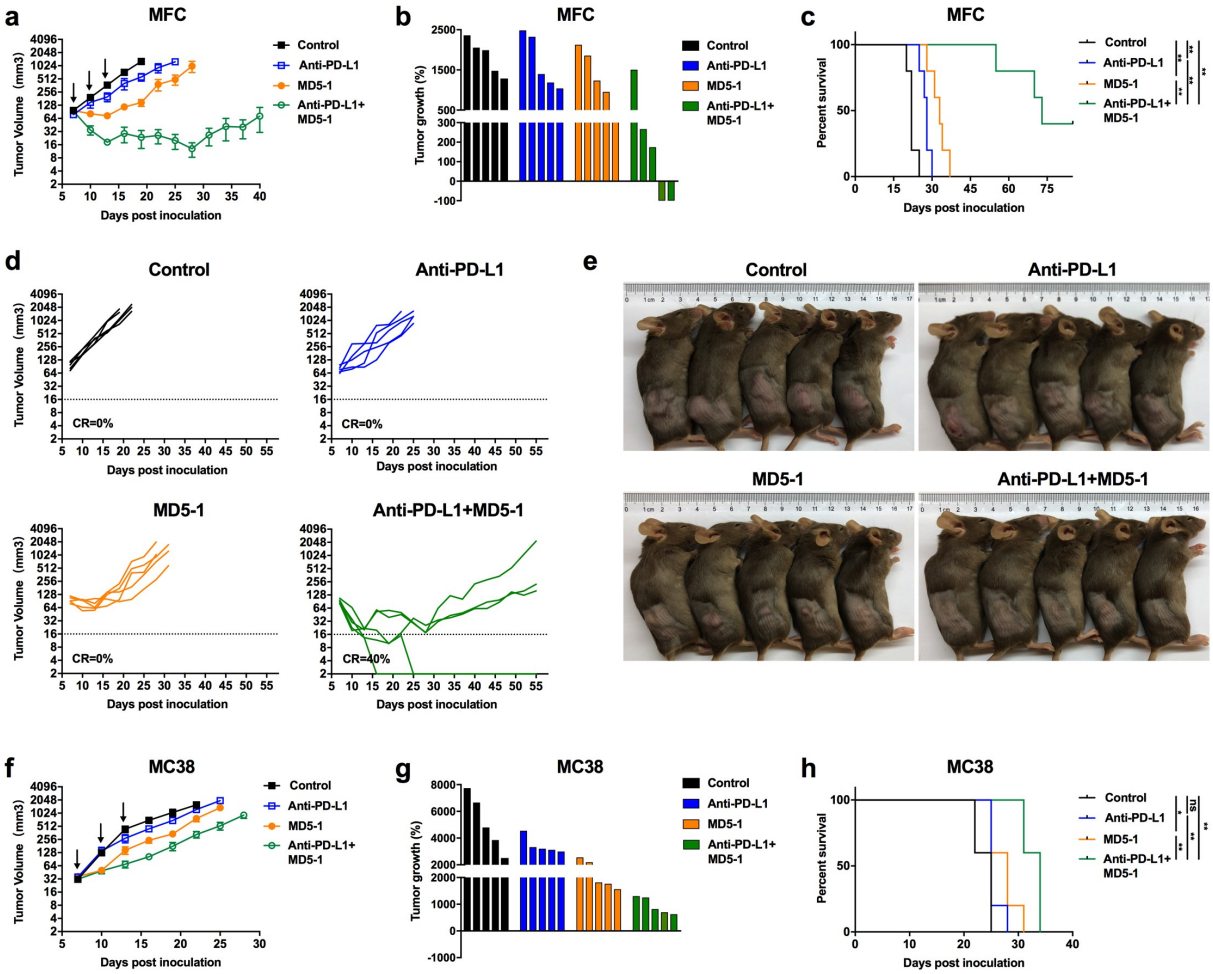

Figure 5. Combination therapy using MD5-1 and anti-PD-L1 antibody is efficacious against MFC and MC38 tumors. 615 mice bearing MFC tumors and C57BL/6 mice bearing MC38 tumors were treated with control IgG, anti-PD-L1 mAb (200 μg/mouse), MD5-1 (50 μg /mouse), or MD5-1 plus anti-PD-L1 mAb. Mice were monitored for tumor growth and survival (n = 5 mice/group). (a) MFC tumor growth summary curves. Black arrows indicate time of treatments. (b) Change in tumor volume compared to baseline. (c) Survival curves of 615 mice. (d) Individual MFC tumor growth curves demonstrating long-term growth kinetics for each treatment. Percent complete response (CR) of each treatment are shown. (e) Images of 615 mice from each treatment group 6 d after drug withdrawal. (f) MC38 tumor growth summary curves. Black arrows indicate time of treatments. (g) Change in tumor volume compared to baseline. (h) Survival curves of C57BL/6 mice. Data are shown as mean ± SEM. Results are representative of 3 independent experiments. Survival curves were analyzed via Mantel-Cox log-rank test, $^{*}p < .05$, $^{**}p < .01$, ns, not significant.

with anti-PD-L1 antibody significantly delayed tumor growth and markedly improved the survival of tumor-bearing mice (Figure 5f-h).

In further experiments, we examined whether the combination therapy induced immune memory in CR 615 mice. Three months after the combination therapy, the CR mice were re-challenged with the same MFC cells. No tumor regrowth was observed in any of the CR mice after MFC cell reinjection. Meanwhile, the age-matched naive mice rapidly developed tumors after MFC cell inoculation (**Supplementary Fig. 8A&B**), indicating that the combination therapy can induce the generation of durable tumor-specific immune memory. Taken together, our results demonstrate that the combination of MD5-1 and anti-PD-L1 antibody is efficacious against gastric cancer and colon cancer.

Combination treatment enhances CD8$^+$ T-cell infiltration and activation in the tumor tissues

In order to determine whether the enhanced antitumor effect by combination of MD5-1 and anti-PD-L1 antibody was associated with improved immune responses, tumor-infiltrating lymphocytes, and myeloid cells of treated MFC tumor-bearing mice were examined by flow cytometry. Compared to MD5-1 or anti-PD-L1 antibody monotherapy, the combination of MD5-1 and anti-PD-L1 antibody significantly increased the frequency of CD8$^+$ T cells in tumor tissues (Figure 6a). The enhanced T-cell infiltration following combination therapy was further confirmed by CD3 staining of the tumor sections (Figure 6b). None of the treatments affected the presence of CD4$^+$ T-regulatory cells (Treg) (Figure 6c), and the combination therapy did not further reduce the tumor MDSC burden compared to MD5-1 monotherapy (Figure 6d), suggesting that MDSC reduction was mainly attributed to the effect of MD5-1. However, with the highest CD8$^+$ T cells frequency, the combination therapy resulted in markedly increased CD8/Treg ratio and CD8/MDSC ratio compared to either monotherapy (Figure 6 e&f). The combination therapy also significantly increased the proportions of IFN-γ and TNF-α producing CD8$^+$ T cells (Figure 6 g&h) and reduced the expression of PD-1 on CD8$^+$ T cells (Figure 6i), suggesting that the tumor-infiltrating CD8$^+$ T cells were more functionally activated and less exhausted. Furthermore, compared to MD5-1 monotherapy, IFN-γ but not TNF-α producing CD4$^+$ T cells were also significantly increased in tumors treated with combination therapy (**Supplementary Fig. 9A&B**).

T lymphocytes were also evaluated in the spleens of treated mice. Although the combination therapy did not significantly increase the proportion of splenic CD8$^+$ T cells (**Supplementary Fig. 10A**), it significantly augmented the percentages of IFN-γ and TNF-α producing CD8$^+$ T cells relative to MD5-1 monotherapy (**Supplementary Fig. 10B&C**). Meanwhile, no significant differences in the frequencies of IFN-γ and TNF-α producing CD4$^+$ T cells were observed between the combination therapy and MD5-1 monotherapy (**Supplementary Fig. 10D&E**). Overall, the combination of MD5-1 and anti-PD-L1 antibody could enhance antitumor immunity by promoting the infiltration and activation of CD8$^+$ T cells.

Combination of MD5-1 and anti-PD-L1 antibody is well tolerated by the mice

Throughout the course of therapy, although mice received the combination treatment experienced certain weight loss, none of the treated mice lost more than 10% of its initial body weight (Figure 7a). Moreover, no obvious pathological alterations were observed in the major organs of the treated mice, including the heart, lung, liver, spleen, and kidney (Figure 7b). All the serological indexes of liver, renal, and heart function were within normal ranges (Figure 7c-e). These results indicate that the combination therapy of MD5-1 and anti-PD-L1 antibody is well tolerated by the host without overt systemic toxicity.

Discussion

MDSCs have been demonstrated to play important roles not only in immune suppression but also in immunotherapy resistance of cancer. The expansion and accumulation of immune suppressive MDSCs have been observed in various murine tumor models and cancer patients.[24,25] However, until now, little research has been done to characterize MDSCs in gastric cancer and colon cancer. Our previous studies showed that mobilization of MDSCs contributes to gastric cancer development in IL-1β transgenic mice and inhibition of MDSCs prevents gastric cancer growth.[26,27] However, whether therapeutically targeting MDSCs could enhance the efficacy of PD-1/PD-L1 blockade immunotherapy in gastric cancer and colon cancer remains to be investigated.

In mice bearing MFC gastric cancer and mice bearing MC38 colon cancer, we found that the MDSCs accumulated robustly in the spleens and tumor tissues as early as 7 d after tumor inoculation. Up to now, therapeutic methods that target MDSCs in preclinical studies are often focused on gMDSCs.[28,29] However, in MFC gastric cancer-bearing mice, while the frequencies of gMDSCs were higher than those of mMDSCs in both spleens and tumors, the mMDSC population cannot be overlooked, since it represents about 21% of splenic MDSC population and 31% of tumoral MDSC population, suggesting that targeting only gMDSCs may have limited therapeutic effects in certain tumors.

Many agents have been found to have the capacity of blocking the immune suppression activity of MDSCs,[30,31] among which depletion of MDSCs by anti-Gr-1 antibodies or cytotoxic chemotherapy drugs (such as gemcitabine and 5-fluorouracil) were proved effective to enhance T-cell antitumor response and inhibit tumor growth in preclinical tumor models.[32–35] However, anti-Gr-1 antibodies may also deplete neutrophils since Gr-1 is a general marker for granulocyte. More importantly, Gr-1 antigen is not expressed on human MDSCs. Meanwhile, although some chemotherapy drugs can selectively deplete MDSCs, the clinical benefits of conventional cytotoxic agents are limited for gastric and colon cancer patients. Thus, it is imperative to explore new MDSC-targeting strategies for cancer treatment.

A previous report by Condamine *et al.* showed that due to ER stress response, MDSCs in tumor-bearing mice express high levels of DR5 and targeting DR5 can lead to selective

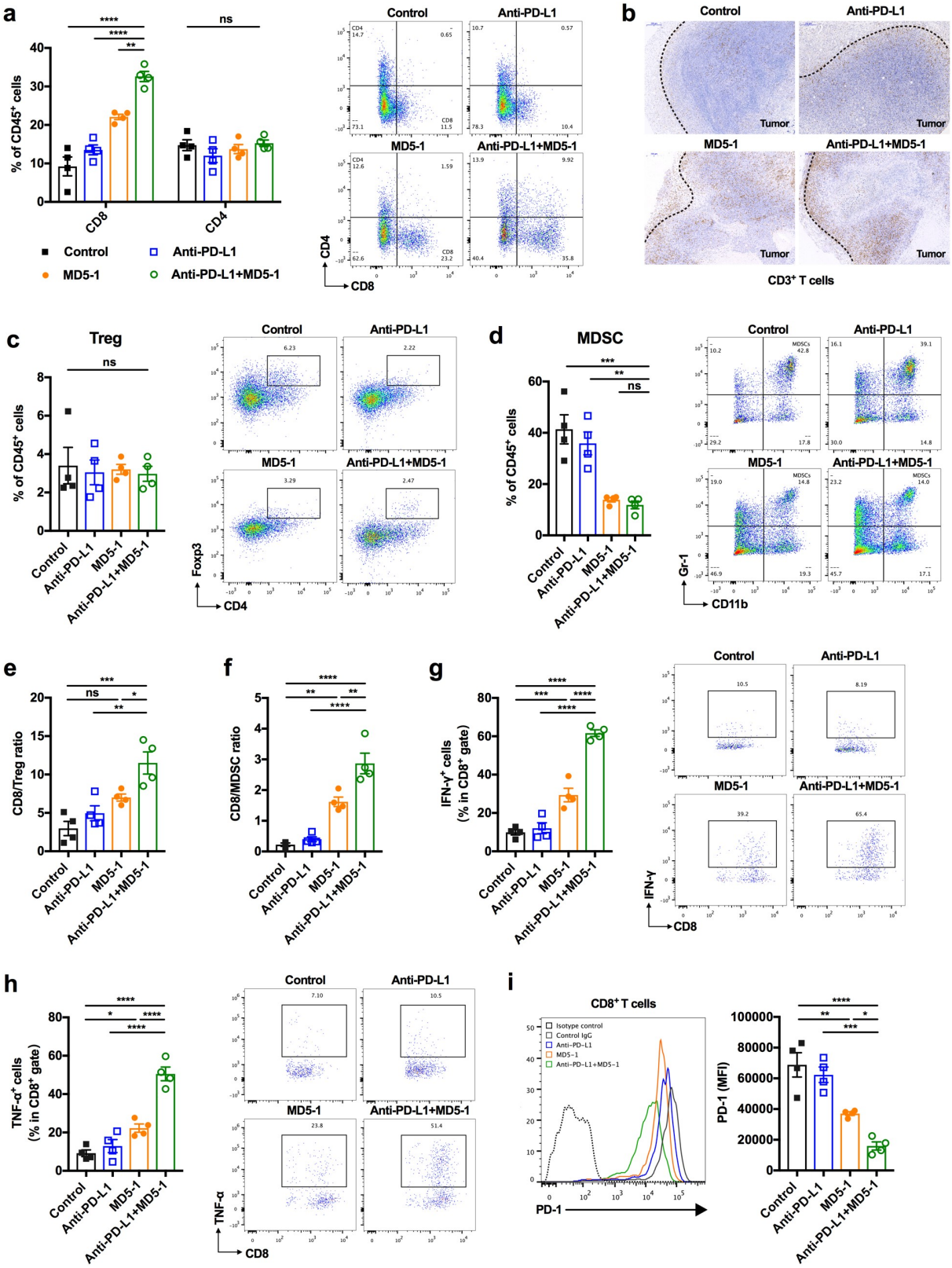

Figure 6. MD5-1 and anti-PD-L1 antibody combination therapy enhances intratumoral $CD8^+$ T-cell infiltration and activation. On d 7 after treatment, MFC tumors of each treated group were isolated and immune cells were analyzed by flow cytometry ($n = 4$ mice/group). (a) Frequencies of tumor-infiltrating $CD8^+$ T cells and $CD4^+$ T cells (left) and representative dot plots gated on live, $CD45^+$ cells (right). (b) Representative tumor-infiltrating $CD3^+$ T cells staining (brown). Dashed line indicates tumor boundary. Scale bar, 200 μm. (c) Frequencies of Treg ($CD4^+Foxp3^+$) in live, $CD45^+$ cells (left) and representative flow cytometry dot plots (right). (d) Frequencies of MDSCs ($CD11b^+Gr\text{-}1^{+}$) in live, $CD45^+$ cells (left) and representative flow cytometry dot plots (right). (e, f) The ratios of $CD8^+$ T cells to Treg (e) and $CD8^+$ T cells to MDSCs (f) in tumors were evaluated. (g, h) Percentages of IFN-γ (g) and TNF-α (h) expressing $CD8^+$ T cells (left) and representative flow cytometry plots (right). (i) Representative histogram plot of PD-1 expressed on $CD8^+$ T cells (left) and quantified surface PD-1 expression of $CD8^+$ T cells (right) in tumors. Data represent at least 2 independent experiments. Data are shown as represent mean ± SEM. *$p < .05$, ** $p < .01$, *** $p < .001$, **** $p < .0001$, ns, not significant by one-way ANOVA with Turkey's multiple comparisons test.

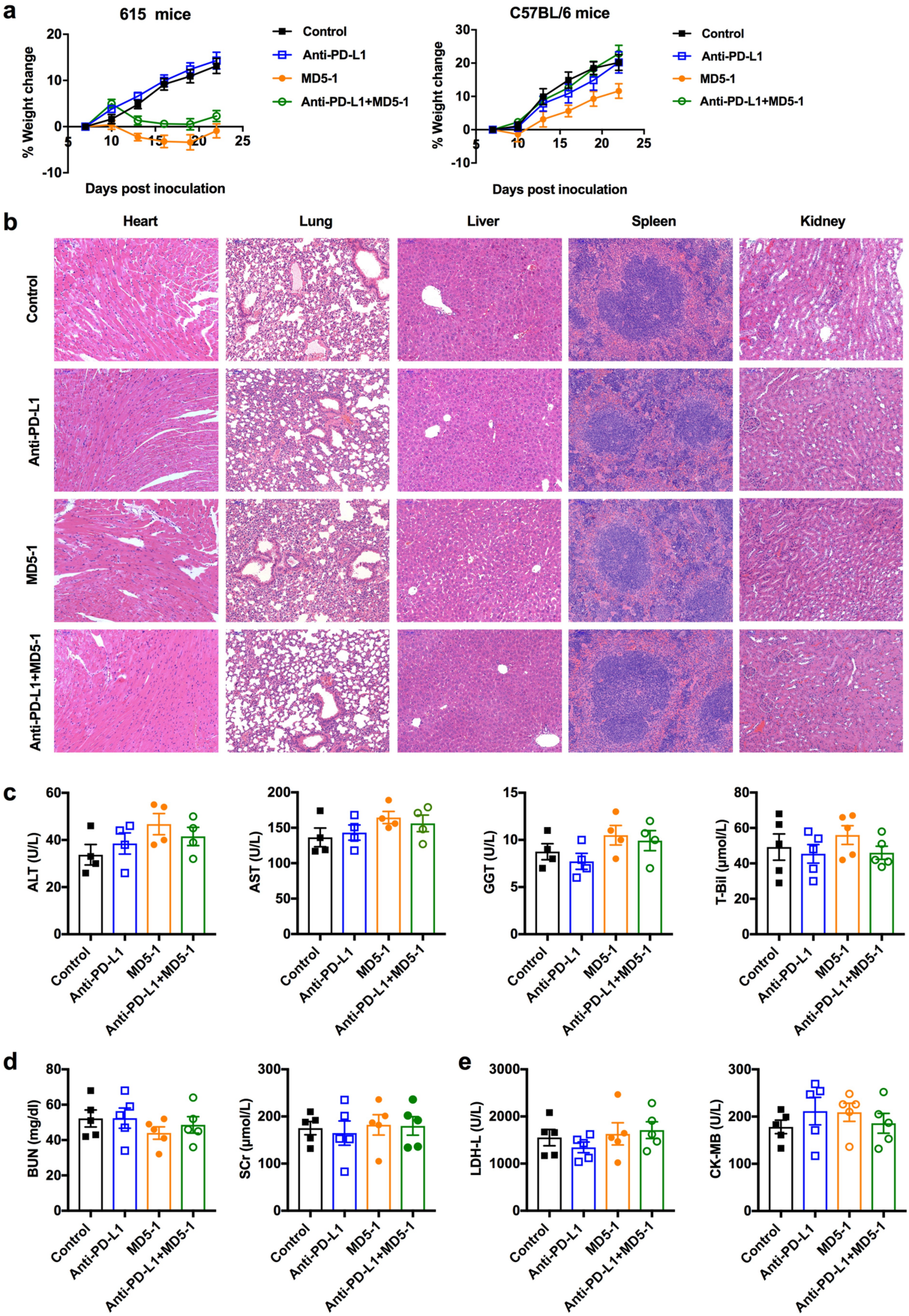

Figure 7. Safety evaluation of MD5-1 and anti-PD-L1 combination therapy. (a) Percent weight changes of tumor-bearing 615 mice (left) and C57BL/6 mice (right) during the course of therapy. are shown. (b) Representative H&E staining images of heart, lung, liver, spleen, and kidney of treated tumor-bearing 615 mice from each treatment group. Scale bar, 100 μm. (c-e) The indexes of liver (c), renal (d) and heart (e) functions in the blood serum of 615 mice at the endpoint of study were measured. $n = 5$ mice/group. Data shown as mean ± SEM.

MDSC elimination.[17] Similarly, we found that MDSCs accumulated in the tumors and spleens of both MFC and MC38 tumor-bearing mice expressed high levels of surface DR5. In MFC tumor-bearing mice, the treatment of agonistic anti-DR5 antibody MD5-1 effectively reduced the MDSC burden without notable cytotoxicity on T cells nor affecting the presence of macrophages and DCs in the tumor microenvironment. Importantly, MD5-1 showed stronger MDSC depletion effect in the tumor tissue than that in the spleen, given that both MDSC subsets in the tumor tissue had higher DR5 expression than their respective counterparts in the spleen. Moreover, in tumor tissue, the depleting effect by MD5-1 was more prominent on mMDSCs than on gMDSCs, mostly because the DR5 expression on mMDSCs was 2.9 times higher than that on gMDSCs. This is an essential observation of our study since the study by Condamine *et al*. mainly emphasized this MDSC-targeting strategy for the depletion of gMDSCs. Thus, determining the ratio between gMDSCs and mMDSCs in patients with gastric or colon cancer could be important for DR5-targeting treatment.

One major characteristic of MDSCs is their ability to inhibit T-cell antitumor activity. Here, we showed that MD5-1-mediated antitumor effect was stronger in immune-competent 615 mice than in T-cell-deficient nude mice. The enhanced tumor-inhibiting effect in 615 mice by MD5-1 treatment was associated with an increased intratumoral and splenic $CD8^+$ T-cell infiltration. Furthermore, the antitumor effect of MD5-1 was markedly blunted by MDSC adoptive transfer. Altogether, these results indicate that MDSC elimination is essential for the antitumor efficacy of MD5-1. However, given that MD5-1 also recognizes DR5 expressing tumor cells, it is possible that the enhanced antitumor immunity is a combinatorial result of MD5-1 targeting MFC tumor and MDSCs. Because MD5-1-mediated tumor killing can also promote tumor-specific effector T cells through the help of antigen presenting cells.[36–38] Thus, characterizing DR5 expression on both tumor cells and MDSCs could better predicate the activation of antitumor immunity after DR5-targeting therapy.

Considering the pivotal role of MDSCs in T-cell suppression, targeting MDSCs represents a promising strategy to improve the efficacy of PD-1/PD-L1 blockade therapy.[39,40] In this study, we demonstrated that targeting DR5 using MD5-1 effectively reduced the MDSC burden in the tumor and remarkably increased the intratumoral $CD8^+$ T-cell infiltration, turning the relative "cold" MFC tumors into "hot." Although MD5-1 therapy alone induced immune activation was insufficient to cause complete tumor regression, it significantly sensitized MFC tumors to anti-PD-L1 therapy. The combination of MD5-1 and anti-PD-L1 antibody was therapeutically superior to either single-agent treatment, led to 40% of complete tumor regression and a markedly prolonged survival of MFC tumor-bearing mice. Moreover, all mice experienced complete tumor regression rejected the re-injection of the same MFC cells, indicating that the combination therapy elicited tumor-specific immune memory. The enhanced antitumor efficacy of the combination therapy was also observed in mice bearing MC38 tumors, suggesting the general applicability of the combination regimen in gastrointestinal cancer. In addition, a recent study by Mondal et al. also showed that DR5 antibodies lead to PD-L1 stabilization on tumor cells and demonstrated the synergistic antitumor effect of co-targeting DR5 and PD-L1 in a murine model of ovarian cancer.[41] However, although MD5-1 effectively enhanced the antitumor effect of anti-PD-L1 therapy in MC38 tumors, no complete tumor regression was observed after the combination therapy. The impaired synergistic efficacy of the combination therapy in MC38 tumors may be attributed to the insensitivity of MC38 cells to MD5-1 induced apoptosis, since a lower tumor burden has a positive effect on anticancer immunity and indicates a better response to immunotherapy.[42,43] Given that many tumor cells develop a certain inherent resistance to TRAIL or anti-DR5 antibody-induced apoptosis irrespective of DR5 expression level such as MC38 cells in our study,[44] evaluation of the sensitivity of tumor cells to agonistic anti-DR5 antibody-induced apoptosis may also better stratify patients that will respond to this form of combination therapy. Moreover, the reason that the agonistic effect of anti-DR5 antibodies requires Fc receptors that are expressed on tumor cells and innate immune cells may also explain why the antitumor effect of these antibodies varies in different tumor-bearing individuals.[15,38]

The enhanced antitumor effect following the combination therapy was concomitant with not only stronger $CD8^+$ T-cell infiltration but also augmented $CD8^+$ T-cell activities as assessed by flow cytometry analysis. We also detected a significantly increased CD8/Treg ratio and decreased PD-1 expression on $CD8^+$ T cells which had been shown to indicate a better response to anti-PD-L1 immunotherapy.[45,46] These results suggested that the combination of DR5-targeting and PD-L1 blockade therapy has remarkable immunomodulatory activity and antitumor efficacy for the treatment of gastric and colon cancers.

The toxicity and safety of agonistic anti-DR5 antibody or anti-PD-L1 antibody single-agent therapy have been properly assessed in many studies.[3,15,47] Here, by using syngeneic mouse models, we assessed the potential toxicities associated with combinatorial treatment with the two agents, which to our knowledge, has not been reported in any published data. We observed no significant pathological and serological changes in major organs of mice that received either single-agent treatment or combination treatment. Notably, the liver function was not affected by MD5-1 used alone or in combination with anti-PD-L1 antibody, as stimulation of DR5 is potentially cytotoxic to hepatocytes.[48,49] Nevertheless, we did observe a certain weight loss in mice treated with MD5-1 single-agent and combinational treatment, however, no mice lost more than 10% of its initial body weight, indicating that MD5-1 monotherapy and combination therapy are well tolerated by the host. Overall, these results provided promising preclinical evidence that a therapeutic strategy that combines agonistic anti-DR5 antibody and anti-PD-L1 antibody may be safe in humans for gastric and colon cancer treatment.

Ultimately, this study for the first time demonstrated that depleting MDSCs through targeting DR5 can effectively overcome MDSC-mediated T-cell suppression and potentiate PD-L1 blockade therapy in gastric and colon tumor-bearing mice, thereby offering a viable approach for the treatment of human gastric and colon cancers. To enhance the translational value of

this study, the antitumor efficacy of this form of combination therapy may need further evaluation in humanized mice models. Furthermore, while anti-PD-L1 antibodies are available clinically and humanized anti-DR5 antibodies have been tested in many clinical trials for the treatment of cancer, it is feasible to translate these preclinical results into early-phase human clinical trials.

Acknowledgments

This project was supported by the National Natural Science Foundation of China under Grant 817732598 and 81472727, the Science and Technology Commission of Shanghai Municipality under Grant 22ZR1438300 and 22140901800, and the Chinese Society of Clinical Oncology Foundation under Grant Y-Q201802-073 and Y-XD202001-0318.

Disclosure statement

No potential conflict of interest was reported by the author(s).

Funding

This work was supported by the Chinese Society of Clinical Oncology [Y-Q201802-073, Y-XD202001-0318.]; National Natural Science Foundation of China [817732598, 81472727]; Shanghai Science and Technology Committee [22ZR1438300, 22140901800].

Ethics approval

All animal experiments were approved by the Animal Care and Use Committee at the Renji Hospital affiliate of Shanghai Jiao Tong University, School of Medicine.

References

1. Sun JY, Lu XJ. Cancer immunotherapy: current applications and challenges. Cancer Lett. 2020;480:1–3. doi:10.1016/j.canlet.2020.03.024.
2. Ribas A, Wolchok JD. Cancer immunotherapy using checkpoint blockade. Science. 2018;359:1350–1355. doi:10.1126/science.aar4060.
3. Brahmer JR, Tykodi SS, Chow LQ, Hwu WJ, Topalian SL, Hwu P, Drake CG, Camacho LH, Kauh J, Odunsi K, et al. Safety and activity of anti-PD-L1 antibody in patients with advanced cancer. N Engl J Med. 2012;366:2455–2465. doi:10.1056/NEJMoa1200694.
4. Janjigian YY, Shitara K, Moehler M, Garrido M, Salman P, Shen L, Wyrwicz L, Yamaguchi K, Skoczylas T, Campos Bragagnoli A, et al. First-line nivolumab plus chemotherapy versus chemotherapy alone for advanced gastric, gastro-oesophageal junction, and oesophageal adenocarcinoma (CheckMate 649): a randomised, open-label, phase 3 trial. Lancet. 2021;398(10294):27–40. doi:10.1016/S0140-6736(21)00797-2.
5. Marvel D, Gabrilovich DI. Myeloid-derived suppressor cells in the tumor microenvironment: expect the unexpected. J Clin Invest. 2015;125:3356–3364. doi:10.1172/JCI80005.
6. Gabrilovich DI, Ostrand-Rosenberg S, Bronte V. Coordinated regulation of myeloid cells by tumours. Nat Rev Immunol. 2012;12(4):253–268. doi:10.1038/nri3175.
7. Loeuillard E, Yang J, Buckarma E, Wang J, Liu Y, Conboy C, Pavelko KD, Li Y, O'Brien D, Wang C, et al. Targeting tumor-associated macrophages and granulocytic myeloid-derived suppressor cells augments PD-1 blockade in cholangiocarcinoma. J Clin Invest. 2020;130(10):5380–5396. doi:10.1172/JCI137110.
8. Lu W, Yu W, He J, Liu W, Yang J, Lin X, Zhang Y, Wang X, Jiang W, Luo J, et al. Reprogramming immunosuppressive myeloid cells facilitates immunotherapy for colorectal cancer. EMBO Mol Med. 2021;13(1):e12798. doi:10.15252/emmm.202012798.
9. Li R, Salehi-Rad R, Crosson W, Momcilovic M, Lim RJ, Ong SL, Huang ZL, Zhang T, Abascal J, Dumitras C, et al. Inhibition of granulocytic myeloid-derived suppressor cells overcomes resistance to immune checkpoint inhibition in LKB1-deficient non-small cell lung cancer. Cancer Res. 2021;81:3295–3308. doi:10.1158/0008-5472.CAN-20-3564.
10. Tobin RP, Jordan KR, Robinson WA, Davis D, Borges VF, Gonzalez R, Lewis KD, McCarter MD. Targeting myeloid-derived suppressor cells using all-trans retinoic acid in melanoma patients treated with Ipilimumab. Int Immunopharmacol. 2018;63:282–291. doi:10.1016/j.intimp.2018.08.007.
11. Holmgaard RB, Zamarin D, Lesokhin A, Merghoub T, Wolchok JD. Targeting myeloid-derived suppressor cells with colony stimulating factor-1 receptor blockade can reverse immune resistance to immunotherapy in indoleamine 2,3-dioxygenase-expressing tumors. EBioMedicine. 2016;6:50–58. doi:10.1016/j.ebiom.2016.02.024.
12. Wesolowski R, Markowitz J, Carson WE 3rd. Myeloid derived suppressor cells – a new therapeutic target in the treatment of cancer. J Immunother Cancer. 2013;1:10. doi:10.1186/2051-1426-1-10.
13. Wu GS, Burns TF, Zhan Y, Alnemri ES, El-Deiry WS. Molecular cloning and functional analysis of the mouse homologue of the KILLER/DR5 tumor necrosis factor-related apoptosis-inducing ligand (TRAIL) death receptor. Cancer Res. 1999;59:2770–2775.
14. Kelley SK, Ashkenazi A. Targeting death receptors in cancer with Apo2L/TRAI. Curr Opin Pharmacol. 2004;4:333–339 doi:10.1016/j.coph.2004.02.006.
15. Li F, Ravetch JV. Apoptotic and antitumor activity of death receptor antibodies require inhibitory Fcγ receptor engagement. Proc Natl Acad Sci U S A. 2012;109: 10966–10971. doi:10.1073/pnas.1208698109.
16. Motoki K, Mori E, Matsumoto A, Thomas M, Tomura T, Humphreys R, Albert V, Muto M, Yoshida H, Aoki M, et al. Enhanced apoptosis and tumor regression induced by a direct agonist antibody to tumor necrosis factor-related apoptosis-inducing ligand receptor 2. Clin Cancer Res. 2005;11:3126–3135. doi:10.1158/1078-0432.CCR-04-1867.
17. Condamine T, Kumar V, Ramachandran IR, Youn JI, Celis E, Finnberg N, El-Deiry WS, Winograd R, Vonderheide RH, English NR, et al. ER stress regulates myeloid-derived suppressor cell fate through TRAIL-R-mediated apoptosis. J Clin Invest. 2014;124:2626–2639. doi:10.1172/JCI74056.
18. Dominguez GA, Condamine T, Mony S, Hashimoto A, Wang F, Liu Q, Forero A, Bendell J, Witt R, Hockstein N, et al. Selective targeting of myeloid-derived suppressor cells in cancer patients Using DS-8273a, an agonistic TRAIL-R2 Antibody. Clin Cancer. 2017;23:2942–2950. doi:10.1158/1078-0432.CCR-16-1784.
19. Urakawa S, Yamasaki M, Goto K, Haruna M, Hirata M, Morimoto-Okazawa A, Kawashima A, Iwahori K, Makino T, Kurokawa Y, et al. Peri-operative monocyte count is a marker of poor prognosis in gastric cancer: increased monocytes are a characteristic of myeloid-derived suppressor cells. Cancer Immunol Immunother. 2019;68(8):1341–1350. doi:10.1007/s00262-019-02366-0.
20. Gabitass RF, Annels NE, Stocken DD, Pandha HA, Middleton GW. Elevated myeloid-derived suppressor cells in pancreatic, esophageal and gastric cancer are an independent prognostic factor and are associated with significant elevation of the Th2 cytokine interleukin-13. Cancer Immunol Immunother. 2011;60:1419–1430. doi:10.1007/s00262-011-1028-0.
21. Wang L, Chang EW, Wong SC, Ong SM, Chong DQ, Ling KL. Increased myeloid-derived suppressor cells in gastric cancer correlate with cancer stage and plasma S100A8/A9 proinflammatory proteins. J Immunol. 2013;190:794–804. doi:10.4049/jimmunol.1202088.
22. Kobayashi M, Chung JS, Beg M, Arriaga Y, Verma U, Courtney K, Mansour J, Haley B, Khan S, Horiuchi Y, et al. Blocking monocytic myeloid-derived suppressor cell function via anti-DC-HIL

/GPNMB antibody restores the in vitro integrity of T cells from cancer patients. Clin Cancer Res. 2019;25:828–838. doi:10.1158/1078-0432.CCR-18-0330.
23. Wu L, Xu Y, Zhao H, Zhou Y, Chen Y, Yang S, Lei J, Zhang J, Wang J, Wu Y, et al. FcγRIIB potentiates differentiation of myeloid-derived suppressor cells to mediate tumor immunoescape. Theranostics. 2022;12:842–858. doi:10.7150/thno.66575.
24. Davis RJ, Moore EC, Clavijo PE, Friedman J, Cash H, Chen Z, Silvin C, Van Waes C, Allen C. Anti-PD-L1 Efficacy can be enhanced by inhibition of myeloid-derived suppressor cells with a selective inhibitor of PI3Kdelta/gamma. Cancer Res. 2017;77:2607–2619. doi:10.1158/0008-5472.CAN-16-2534.
25. De Cicco P, Ercolano G, Ianaro A. The new era of cancer immunotherapy: targeting myeloid-derived suppressor cells to overcome immune evasion. Front Immunol. 2020;11:1680. doi:10.3389/fimmu.2020.01680.
26. Tu SP, Jin H, Shi JD, Zhu LM, Suo Y, Lu G, Liu A, Wang TC, Yang CS. Curcumin induces the differentiation of myeloid-derived suppressor cells and inhibits their interaction with cancer cells and related tumor growth. Cancer Prev Res (Phila). 2012;5:205–215. doi:10.1158/1940-6207.CAPR-11-0247.
27. Tu S, Bhagat G, Cui G, Takaishi S, Kurt-Jones EA, Rickman B, Betz KS, Penz-Oesterreicher M, Bjorkdahl O, Fox JG, et al. Overexpression of interleukin-1beta induces gastric inflammation and cancer and mobilizes myeloid-derived suppressor cells in mice. Cancer Cell. 2008;14:408–419. doi:10.1016/j.ccr.2008.10.011.
28. Kim K, Skora AD, Li Z, Liu Q, Tam AJ, Blosser RL, Diaz LA Jr, Papadopoulos N, Kinzler KW, Vogelstein B, et al., Eradication of metastatic mouse cancers resistant to immune checkpoint blockade by suppression of myeloid-derived cells. Proc Natl Acad Sci U S A. 2014;111: 11774–11779. doi:10.1073/pnas.1410626111.
29. Chen HM, van der Touw W, Wang YS, Kang K, Mai S, Zhang J, Alsina-Beauchamp D, Duty JA, Mungamuri SK, Zhang B, et al. Blocking immunoinhibitory receptor LILRB2 reprograms tumor-associated myeloid cells and promotes antitumor immunity. J Clin Invest. 2018;128:5647–5662. doi:10.1172/JCI97570.
30. Li T, Liu T, Zhu W, Xie S, Zhao Z, Feng B, Guo H, Yang R. Targeting MDSC for immune-checkpoint blockade in cancer Immunotherapy: current progress and new prospects. Clin Med Insights Oncol. 2021;15:11795549211035540. doi:10.1177/11795549211035540.
31. Orillion A, Hashimoto A, Damayanti N, Shen L, Adelaiye-Ogala R, Arisa S, Chintala S, Ordentlich P, Kao C, Elzey B, et al. Entinostat neutralizes myeloid-derived suppressor cells and enhances the antitumor effect of PD-1 inhibition in murine models of lung and renal cell carcinoma. Clin Cancer Res. 2017;23:5187–5201. doi:10.1158/1078-0432.CCR-17-0741.
32. Vincent J, Mignot G, Chalmin F, Ladoire S, Bruchard M, Chevriaux A, Martin F, Apetoh L, Rébé C, Ghiringhelli F. 5-Fluorouracil selectively kills tumor-associated myeloid-derived suppressor cells resulting in enhanced T cell-dependent antitumor immunity. Cancer Res. 2010;70:3052–3061. doi:10.1158/0008-5472.CAN-09-3690.
33. Suzuki E, Kapoor V, Jassar AS, Kaiser LR, Albelda SM. Gemcitabine selectively eliminates splenic Gr-1+/CD11b+ myeloid suppressor cells in tumor-bearing animals and enhances antitumor immune activity. Clin Cancer Res. 2005;11:6713–6721. doi:10.1158/1078-0432.CCR-05-0883.
34. Seung LP, Rowley DA, Dubey P, Schreiber H. Synergy between T-cell immunity and inhibition of paracrine stimulation causes tumor rejection. Proc Natl Acad Sci U S A. 1995;92;6254–6258. doi:10.1073/pnas.92.14.6254.
35. Srivastava MK, Zhu L, Harris-White M, Kar UK, Huang M, Johnson MF, Lee JM, Elashoff D, Strieter R, Dubinett S, et al. Myeloid suppressor cell depletion augments antitumor activity in lung cancer. PLoS One. 2012;7:e40677. doi:10.1371/journal.pone.0040677.
36. Tsukita Y, Okazaki T, Ebihara S, Komatsu R, Nihei M, Kobayashi M, Hirano T, Sugiura H, Tamada T, Tanaka N, et al. Beneficial effects of sunitinib on tumor microenvironment and immunotherapy targeting death receptor5. Oncoimmunology. 2019;8:e1543526. doi:10.1080/2162402X.2018.1543526.
37. Takeda K, Yamaguchi N, Akiba H, Kojima Y, Hayakawa Y, Tanner JE, Sayers TJ, Seki N, Okumura K, Yagita H, et al. Induction of tumor-specific T cell immunity by anti-DR5 antibody therapy. J Exp Med. 2004;199:437–448. doi:10.1084/jem.20031457.
38. Haynes NM, Hawkins ED, Li M, McLaughlin NM, Hämmerling GJ, Schwendener R, Winoto A, Wensky A, Yagita H, Takeda K, et al. CD11c+ dendritic cells and B cells contribute to the tumoricidal activity of anti-DR5 antibody therapy in established tumors. J Immunol. 2010;185:532–541. doi:10.4049/jimmunol.0903624.
39. Liu M, Zhou J, Liu X, Feng Y, Yang W, Wu F, Cheung OK, Sun H, Zeng X, Tang W, et al. Targeting monocyte-intrinsic enhancer reprogramming improves immunotherapy efficacy in hepatocellular carcinoma. Gut. 2020;69:365–379. doi:10.1136/gutjnl-2018-317257.
40. Flores-Toro JA, Luo D, Gopinath A, Sarkisian MR, Campbell JJ, Charo IF, Singh R, Schall TJ, Datta M, Jain RK, et al. CCR2 inhibition reduces tumor myeloid cells and unmasks a checkpoint inhibitor effect to slow progression of resistant murine gliomas. Proc Natl Acad Sci U S A. 2020;117(2):1129–1138. doi:10.1073/pnas.1910856117.
41. Mondal T, Shivange GN, Tihagam RG, Lyerly E, Battista M, Talwar D, Mosavian R, Urbanek K, Rashid NS, Harrell JC, et al. Unexpected PD-L1 immune evasion mechanism in TNBC, ovarian, and other solid tumors by DR5 agonist antibodies. EMBO Mol Med. 2021;13:e12716. doi:10.15252/emmm.202012716.
42. Kim SI, Cassella CR, Byrne KT. Tumor burden and immunotherapy: impact on immune infiltration and therapeutic outcomes. Front Immunol. 2020;11:629722. doi:10.3389/fimmu.2020.629722.
43. Dall'Olio FG, Marabelle A, Caramella C, Garcia C, Aldea M, Chaput N, Robert C, Besse B. Tumour burden and efficacy of immune-checkpoint inhibitors. Nat Rev Clin Oncol. 2022;19:75–90. doi:10.1038/s41571-021-00564-3.
44. Dubuisson A, Micheau O. Antibodies and Derivatives Targeting DR4 and DR5 for Cancer Therapy. Antibodies (Basel). 2017;6(4):16. doi:10.3390/antib6040016.
45. Kim H, Kwon HJ, Han YB, Park SY, Kim ES, Kim SH, Kim YJ, Lee JS, Chung JH. Increased CD3+ T cells with a low FOXP3+/CD8+ T cell ratio can predict anti-PD-1 therapeutic response in non-small cell lung cancer patients. Mod Pathol 2019;32:367–375. doi:10.1038/s41379-018-0142-3.
46. Ngiow SF, Young A, Jacquelot N, Yamazaki T, Enot D, Zitvogel L, Smyth MJ. A threshold level of intratumor CD8+ T-cell PD1 expression dictates therapeutic response to anti-PD1. Cancer Res. 2015;75:3800–3811. doi:10.1158/0008-5472.CAN-15-1082.
47. Wang DY, Salem JE, Cohen JV, Chandra S, Menzer C, Ye F, Zhao S, Das S, Beckermann KE, Ha L, et al. Fatal toxic effects associated with immune checkpoint inhibitors: a systematic review and meta-analysis. JAMA Oncology. 2018;4:1721–1728. doi:10.1001/jamaoncol.2018.3923.
48. Jo M, Kim TH, Seol DW, Esplen JE, Dorko K, Billiar TR, Strom SC. Apoptosis induced in normal human hepatocytes by tumor necrosis factor-related apoptosis-inducing ligand. Nat Med. 2000;6:564–567. doi:10.1038/75045.
49. Corazza N, Jakob S, Schaer C, Frese S, Keogh A, Stroka D, Kassahn D, Torgler R, Mueller C, Schneider P, et al. TRAIL receptor-mediated JNK activation and Bim phosphorylation critically regulate Fas-mediated liver damage and lethality. J Clin Invest. 2006;116:2493–2499. doi:10.1172/JCI27726.